Ferromagnetic ground state of SU(3) Hubbard model on the Lieb lattice

Wenxing Nie and Deping Zhang
Institute for Advanced Study, Tsinghua University, Beijing, 100084, China

Wei Zhang*
Department of Physics, Renmin University of China, Beijing 100872, China and
Beijing Key Laboratory of Opto-electronic Functional Materials and Micro-nano Devices,
Renmin University of China, Beijing 100872, China
(Dated: August 9, 2016)

We investigate the magnetic properties of the ground state of the repulsive fermionic SU(3) Hubbard model on the Lieb lattice from weak to strong interactions, by means of mean-field approximation. To see how well the mean-field method works, we first study the magnetic properties of the ground state of SU(2) Hubbard model at the mean-field level, and find that our results are consistent with known rigorous theorems. We then extend the mean-field calculation for Hubbard model with SU(3) symmetry. We find that, at 4/9 filling, SU(3) symmetry spontaneously breaks into SU(2)×U(1) symmetry in the ground state, resulting in a staggered ferromagnetic state for any U at zero temperature. At finite temperature, the long-range order is absent by Mermin-Wagner theorem. However, the quasi long-range magnetic order may exist. Our mean-field calculation estimate the quasi long-range order is destroyed by thermal fluctuation, but it can persist up to a finite temperature. These results are relevant to current experiments with fermionic alkaline-earth (-like) atoms loaded into optical lattice, and could be observed in experiments.

PACS numbers: 71.10.Fd, 71.27.+a, 67.85.-d

arXiv:1607.08618v2 [cond-mat.str-el] 8 Aug 2016

I. INTRODUCTION

The investigation of itinerant ferromagnetism is one of the fundamental and central topics in theoretical condensed matter physics [1–8]. Although itinerant ferromagnetism is generally considered as a result of strong electron-electron interaction since paramagnetism is an inevitable consequence of the Pauli exclusion principle in non-interacting many-electron systems, strong interaction does not necessarily lead to ferromagnetism. For instance, Lieb and Mattis proved that ferromagnetism never happens in one-dimensional systems with only nearest neighbor hopping, no matter how strong the interaction is [1]. Therefore, ferromagnetism of itinerant electrons is still a challenging problem in condensed matter physics, due to the subtle interplay between the kinetic energy and interacting energy, from where various interesting phenomena emerge, e.g., superconductivity and quantum Hall effect.

Due to the subtle sign problem of fermions, rigorous proofs for ferromagnetism of fermionic Hubbard model are very rare [2–8]. The only existing fews hence play important roles as benchmarks for the magnetic properties of the ground state, and can hint us the possible ways to realize the ferromagnetic ground state. One of the earliest rigorous proofs of itinerant ferromagnetism is attributed to Thouless [9] and Nagaoka [2]. It is shown that, with *infinite* on-site repulsion and single hole away from half filling, the ground state of the Hubbard model defined on a lattice satisfying connectivity condition is unique with saturated ferromagnetism (with maximal total spin $S = N_e/2$, where N_e is the number of electrons). In 1989, Lieb proved that on a general bipartite lattice with the two sublattices having different numbers of sites, the ground state of the Hubbard model at half filling with any *finite* repulsion is an unsaturated ferromagnetic state, which is also referred as a ferrimagnetic state with total spin being proportional to system size, $S = \big||\Lambda_{\rm A}| - |\Lambda_{\rm B}|\big|/2$, where $|\Lambda_{\rm A(B)}|$ is the number of sites on sublattice A (B) [7]. In such a setting, a consequence of bipartite condition is the existence of a non-dispersive, or equivalently, a flat band within the single-electron spectrum. Such a non-dispersive band implies the existence of localized single-particle eigenstates in real space and degeneracy of the ground state of single-particle spectrum. This type of ferromagnetism is then referred as flat-band ferromagnetism, and is further proved by Mielke and Tasaki [3–6]. The role of flat band for ferromagnetism can be understood in following argument. In a non-interacting system, the ferromagnetic state is one of the many degenerate ground states when particles fill the flat band. As one turns on the interaction between electrons, such degeneracy is lifted by perturbation and the ferromagnetic ground state may be selected out by interaction to be the only ground state. Although the particle-filling-flat-band picture, which only holds in non- and weak-interacting limit, completely breaks down in strongly interacting many-electron system, a lattice featured by a flat band may still be helpful to realize ferromagnetism in interacting systems.

These two seemingly different approaches to realize ferromagnetism, Nagaoka's ferromagnetism [2] and flat-band ferromagnetism [3–7], can be understood in a uni-

* Corresponding author: wzhangl@ruc.edu.cn

fied manner in the context of Stoner's criterion for ferromagnetism: $\rho(E_{\rm F})U > 1$, where $\rho(E_{\rm F})$ is the density of states (DOS) at Fermi level and U is the Coulomb interaction. Although this argument is at the mean-field level, it gives us the picture that there may be an instability towards ferromagnetism when the DOS at the Fermi level and/or the Coulomb interaction is sufficiently large. These theorems mentioned above could be thought as satisfying the condition of Stoner's criterion: either through infinite interaction, or through infinite DOS at the Fermi level.

The rigorous theorems mentioned above are proved for Hubbard model for typical electronic systems, which posses SU(2) spin-rotational symmetry. One interesting question is that what is the magnetic property of the ground state of Hubbard model which posses a higher SU(N) spin-rotational symmetry? SU(N) symmetry was originally introduced in condensed matter physics as a mathematical extension or theoretical tool for SU(2) symmetry of strongly correlated systems[10–13]. However, the degrees of freedom offered by the nuclear spin of cold atoms could give the playground to investigate strongly correlated particles with a higher symmetry. The realization of SU(N) Hubbard in cold atoms has not only been theoretically proposed [14, 15], but also been experimentally realized by loading ultracold alkaline-earth (-like) atoms in various optical lattices [16–21]. The alkaline-earth (-like) atoms are proposed to be the best candidates for the realization of fermions with an SU(N) symmetry, where $N = 2I + 1$ is the number of internal nuclear states and I is the nuclear spin, e.g., strontium atoms ^{87}Sr with $I = 9/2$, and ytterbium atoms ^{171}Yb, ^{173}Yb with $I = 1/2, 5/2$. Recently, the progresses of so-called orbital Feshbach resonance provide the ability to tune the interatomic interaction between alkaline-earth atoms, facilitating the studies of quantum phases in the underlying systems [22–24].

The SU($N > 2$) generalization of itinerant ferromagnetism has been investigated in SU(N) Hubbard model previously [25, 26]. In Ref. 25, a sufficient condition is provided for an extension of Nagaoka state by rigorous proof. In Ref. 26, the transition from paramagnet to itinerant ferromagnet is found and the ferromagnet can be stabilized by increasing the scattering length. Moreover, in Ref. 26, the SU(N) generalization of Stoner's criterion for ferromagnetism was derived at the mean-field level and is found to be the same as in the SU(2) case. Since Nagaoka' theorem and ferromagnetism based on flat band in SU(2) systems could be regarded as satisfying the SU(2) Stoner's criterion, we expect that the generalized SU(N) ferromagnetism is possible in systems which satisfies the SU(N) Stoner's criterion, for example, a system with partially filled flat band, where the DOS diverges at Fermi level.

In this work, we investigate the magnetic property of the ground state of the SU(3) Hubbard model with *finite* repulsion on the Lieb lattice. Lieb lattice has many advantages to investigate this problem. First, with only nearest-neighbor hoppings, Lieb lattice is bipartite and featured by a flat band in the middle of single-electron spectrum. Filling particles to the flat band in non-interacting picture, where the DOS diverges, is helpful to realize the ferromagnetic ground state with *finite* interaction. Second, Lieb lattice is a special lattice structure described by Lieb's theorem, so that we can compare our calculation of SU(2) Hubbard model with rigorous theorem. Last but not least, Lieb lattice has been successfully realized for ultracold ^{173}Yb atoms [20, 21, 27], paving the way for the experimental investigation of flat-band ferromagnetism with SU(N) symmetry. We perform the mean-field calculation to investigate the magnetic properties of the ground state of SU(3) Hubbard model. Although the mean-field theory is not as reliable as rigorous theorems, it does provide us some insights about the possible ferromagnetic ground state, the effect of interaction, and in what temperature regime the quasi long-range magnetic order persists.

The reminder of the paper is organized as follows. We first briefly review the band structure of the tight-binding model on the Lieb lattice in Sec. II. In Sec. III, we define the model with SU(N) symmetry and discuss the symmetry implied by the Hamiltonian. In Sec. IV, we decouple the interaction in spin (or flavor) channel and develop the general mean-field approach for SU(N) Hubbard model. And we discuss the simplifications and implications of the model if the ground state supports collinear magnetic orders. In Sec. V, we present the results of mean-field calculation for SU(2) Hubbard model where the ferromagnetic ground state is found, and compare our results with previous known rigorous theorems. In Sec. VI, we present the results of mean-field calculation for SU(3) Hubbard model at 4/9 filling. We find that the ground state is ferromagnetic, as a consequence of SU(3) symmetry spontaneously breaking into SU(2)×U(1) symmetry. Finally, in Sec. VII, we present the conclusions. The generators of SU(3) group, i.e., the Gell-Mann matrices, and the technical part of mean-field calculation involved are presented in Appendices.

II. TIGHT-BINDING MODEL ON THE LIEB LATTICE

The two-dimensional Lieb lattice is an important building block of layered perovskite material, e.g., the CuO_2 plane in high-T_c cuprate superconductors. It consists of two sublattices as shown in Fig. 1 (a): one sublattice spacing a (labeled in blue), the other spacing $a/\sqrt{2}$ and titling for 45° (labeled in purple). The dotted square in Fig. 1 (a) shows one unit cell, which contains three sites labeled by A, B and C. Without loss of generality, we can assume there are three sublattices and label them as A, B, and C as well, since the magnetization orders could be different on site B and site C when C_4 symmetry is broken. Actually, adding imbalanced chemical potential on different sublattices, the three-fold degeneracy at (π, π)

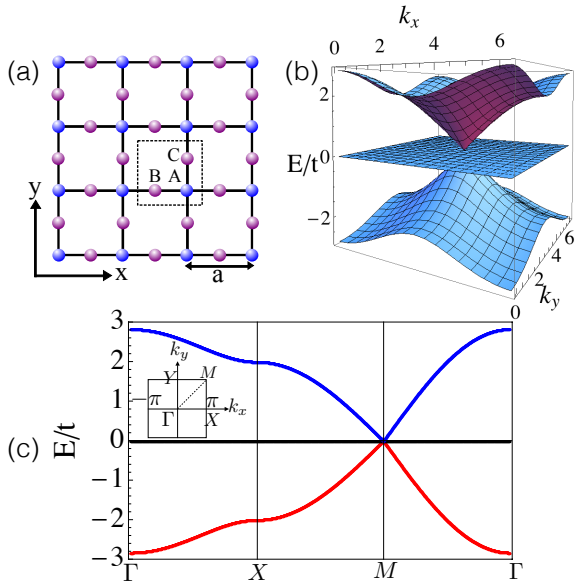

FIG. 1. (a) Lattice structure of the Lieb lattice. The dotted square shows one unit cell, containing three lattice sites with indexes A, B, and C. (b) The band structure of tight-binding model on the Lieb lattice. (c) The band structure along high symmetric lines in the first BZ, in which the inset shows the first BZ and high symmetric points.

point in momentum space is lifted and the ground state supports a nematic phase accompanying the C_4 symmetry breaking [28, 29]. The basis vectors of the unit cell can be chosen as $\mathbf{a}_1 = (a, 0)$ and $\mathbf{a}_2 = (0, a)$.

We start with the spinless tight-binding model on the finite Lieb lattice Λ first:

$$\mathcal{H}_{\rm tb} = -\sum_{\langle i,j\rangle\in\Lambda} (t_{ij} c_i^\dagger c_j + \text{h.c.}), \tag{1}$$

where $\langle i, j\rangle$ runs over all pairs of nearest-neighbor sites on lattice Λ, and $c_i^\dagger$ (c_i) is the creation (annihilation) operator for fermion on site i, satisfying anti-commutation relations $\{c_i^\dagger, c_j\} = \delta_{ij}$ and $\{c_i, c_j\} = 0$. For simplicity, we take the uniform real hopping amplitudes $t_{ij} = t$ and assume $t_{ii} = 0$. With only nearest-neighbor hoppings, Lieb lattice is bipartite and consequently featured by a flat band. The band structure is easily obtained by transforming $\mathcal{H}_{\rm tb}$ into momentum space, $\mathcal{H}_{\rm tb} = \sum_{\mathbf{k}} \Phi_{\mathbf{k}}^\dagger H_{\rm tb}(\mathbf{k}) \Phi_{\mathbf{k}}$, where $\Phi_{\mathbf{k}}$ is a 3-component spinor $(c_{\rm A}(\mathbf{k}), c_{\rm B}(\mathbf{k}), c_{\rm C}(\mathbf{k}))^T$, with sublattice indices A, B, C. The vector $\mathbf{k} = (k_x, k_y)$ belongs to the first Brillouin zone (BZ). The first BZ is shown in the inset of Fig. 1(c). $H_{\rm tb}(\mathbf{k})$ takes the form

$$H_{\rm tb}(\mathbf{k}) = -2t \begin{pmatrix} 0 & \cos(k_x a/2) & \cos(k_y a/2) \\ \cos(k_x a/2) & 0 & 0 \\ \cos(k_y a/2) & 0 & 0 \end{pmatrix}.$$

It has two dispersive bands, and one flat band in the middle of the spectrum: $\epsilon_0(\mathbf{k}) = 0$, $\epsilon_\pm(\mathbf{k}) = \pm t\sqrt{4 + 2\cos(\mathbf{k}\cdot\mathbf{a}_1) + 2\cos(\mathbf{k}\cdot\mathbf{a}_2)}$. These three bands touch each other at M point (π, π) as shown in Figs. 1(b) and 1(c).

Due to the special band structure of the Lieb lattice, its magnetic and topological properties have been comprehensively investigated [26–35]. In experiment, the Lieb lattice can be realized by imposing three types of optical lattices [27, 30, 36, 37], leading to the following potential profile: $V(x, y) = V_0[\sin^2(kx) + \sin^2(ky)] + V_1[\sin^2(2kx) + \sin^2(2ky)] + V_2[\cos^2(kx/2 + ky/2) + \cos^2(kx/2 - ky/2)]$, where $V_0 = V_1 = 2V_2$ and $k = \pi/\lambda$.

III. SU(N) HUBBARD MODEL ON THE LIEB LATTICE

In the following, we consider the Hubbard model with SU(N) spin-rotational symmetry, with the *finite* repulsive on-site density-density interaction $U > 0$. In general, the Hamiltonian can be written as:

$$\mathcal{H} = -t \sum_{\langle i,j\rangle\in\Lambda} \sum_{\alpha=1}^{N} (c_{i,\alpha}^\dagger c_{j,\alpha} + \text{h.c.}) + U \sum_i n_i^2, \tag{2}$$

where α is the label of the flavor or color of a fermion ($\alpha = 1, \cdots, N$, where N is the number of flavors or colors of a fermion). In cold atomic systems, N is the number of degenerate nuclear states. The operator $c_{i,\alpha}$ and its adjoint $c_{i,\alpha}^\dagger$ satisfy the fermionic anticommutation relations $\{c_{i,\alpha}^\dagger, c_{j,\beta}\} = \delta_{ij}\delta_{\alpha\beta}$ and $\{c_{i,\alpha}, c_{j,\beta}\} = 0$. The number operator of fermions at site i is defined as $n_i = \sum_{\alpha=1}^N n_{i,\alpha}$ with $n_{i,\alpha} = c_{i,\alpha}^\dagger c_{i,\alpha}$.

The symmetry of the Hamiltonian Eq. (2) has been discussed in detail in Ref. 25. Besides the trivial conservation of the total number of fermions, the Hamiltonian exhibits a global U(N) = U(1) × SU(N) symmetry. One can construct total number operator and spin operator, which commute with the Hamiltonian Eq. (2):

$$\hat{N} = \sum_{i\in\Lambda} n_i, \tag{3}$$

$$\hat{S}_i^a = \sum_{\alpha,\beta=1}^{N} c_{i\alpha}^\dagger T_{\alpha\beta}^a c_{i\beta} \qquad (a = 1, \cdots, N^2 - 1), \tag{4}$$

where $T^a = \tau^a/2$ are the generators of SU(N) Lie algebra. To be specific, for fermions with SU(2) symmetry, $\alpha = 1, 2$ (or equivalently $\alpha = \uparrow, \downarrow$), and $\tau^a = \sigma^a$ ($a = 1, 2, 3$), where σ^a's are the Pauli matrices. For fermions with SU(3) symmetry, $\alpha = 1, 2, 3$ and $\tau^a = \lambda^a$ ($a = 1, \cdots, 8$), where λ^a's are the Gell-Mann matrices (shown in Appendix A).

For the Hamiltonian Eq. (2) with SU(2) symmetry on the Lieb lattice at half filling, Lieb has proved rigorously the ferromagnetism of the ground state [7]: it is unique (apart from the trivial $(2S+1)$-fold degeneracy) and has total spin $S = \mathcal{N}/2$, where $\mathcal{N}$ is the number of unit

cells. Strictly speaking, it is ferrimagnetism because it is not saturated. Ferromagnetism here in Lieb's terminology means the total spin is nonzero and proportional to systems size. We follow Lieb's terminology and do not distinguish ferrimagnetism from ferromagnetism in the following.

There is no general theorem for ferromagnetism of the Hamiltonian Eq. (2) with SU($N > 2$) symmetry with finite interaction U, as far as we know. For SU(3) Hubbard model with attractive interaction $U < 0$, the spin reflection positivity (the method employed in Lieb's proof for SU(2) Hubbard model) can be extended with the aid of Majorana fermions [38, 39]. However, for repulsive interaction $U > 0$, the extension is not trivial to our knowledge. Therefore, we use Hartree-Fock mean-field approximation for the magnetic properties of the ground state of Hubbard model with SU(2) and SU(3) symmetries, respectively.

IV. GENERAL MEAN-FIELD APPROACH FOR SU(N) HUBBARD MODEL

Before focussing on specific calculation for SU(2) and SU(3) Hubbard models, we present the general mean-field formulae for SU(N) Hubbard model. And then we discuss the simplifications and implications from the general formulae in a special case, when the magnetization vectors are found to be collinear.

With the completeness relation of the generators of SU(N) Lie algebra, the density-density interaction can be decomposed in spin channel (more details in Appendix B):

$$U\sum_i n_i^2 = -\frac{2NU}{N+1}\sum_i \mathbf{S}_i^2 + NU\sum_i n_i, \tag{5}$$

where the SU(N) "spin" operator is constructed in Eq. (4). Perform the mean-field approximation, $\mathbf{S}_i^2 \simeq 2\langle\mathbf{S}_i\rangle\cdot\mathbf{S}_i - \langle\mathbf{S}_i\rangle^2$, and let magnetization $\mathbf{m}_i = \langle\mathbf{S}_i\rangle$, the mean-field Hamiltonian is expressed as

$$\mathcal{H}_{\rm MF} = -t\sum_{\langle i,j\rangle\in\Lambda}\sum_{\alpha=1}^{N}(c_{i\alpha}^\dagger c_{j\alpha} + \text{h.c.}) + \frac{2NU}{N+1}\sum_{i\in\Lambda}\mathbf{m}_i^2 - \frac{4NU}{N+1}\sum_{i\in\Lambda}\sum_{\alpha,\beta=1}^{N} c_{i\alpha}^\dagger \mathbf{m}_i\cdot\frac{\boldsymbol{\tau}_{\alpha\beta}}{2}c_{i\beta}. \tag{6}$$

Assume the translation symmetry is not broken, so that the magnetization orders within each sublattice are uniform. Hence we can do a Fourier transformation, $c_{\mu,\alpha}(\mathbf{k}) = \frac{1}{\sqrt{\mathcal{N}}}\sum_{\mathbf{R}} e^{-i\mathbf{k}\cdot\mathbf{R}}c_{\mu,\alpha}(\mathbf{R})$, where $\mathbf{R}$ is the position of a unit cell, μ = A,B,C labels the sublattices, and $\mathcal{N}$ is the total number of unit cells. We transform the mean-field Hamiltonian into momentum space,

$$\mathcal{H}_{\rm MF} = \sum_{\mathbf{k}}\Phi_{\mathbf{k}}^\dagger H_{\mathbf{k}}^{\rm MF}\Phi_{\mathbf{k}} + \frac{2NU}{N+1}\sum_i \mathbf{m}_i^2, \tag{7}$$

where $\Phi_{\mathbf{k}} = (c_{\mathrm{A},\alpha}(\mathbf{k}), c_{\mathrm{B},\alpha}(\mathbf{k}), c_{\mathrm{C},\alpha}(\mathbf{k}))$ is a $3N$-component spinor with $\alpha = 1,\cdots,N$, and

$$H_{\mathbf{k}}^{\rm MF} = -\begin{pmatrix} \frac{2NU}{N+1}\mathbf{m}_{\rm A}\cdot\boldsymbol{\tau} & t\cos(\frac{k_x a}{2})\mathbb{1} & t\cos(\frac{k_y a}{2})\mathbb{1} \\ t\cos(\frac{k_x a}{2})\mathbb{1} & \frac{2NU}{N+1}\mathbf{m}_{\rm B}\cdot\boldsymbol{\tau} & \mathbf{0} \\ t\cos(\frac{k_y a}{2})\mathbb{1} & \mathbf{0} & \frac{2NU}{N+1}\mathbf{m}_{\rm C}\cdot\boldsymbol{\tau} \end{pmatrix} \tag{8}$$

The magnetization $\mathbf{m}_\mu$ is an (N^2-1)-dimensional vector in spin space, which transforms according to the adjoint representation of SU(N) Lie algebra. The standard mean-field self-consistent calculation goes as follows: start with arbitrary $3(N^2-1)$ parameters of $\mathbf{m}_\mu$, numerically calculate the ground state, obtain the expectation value of spin operator in the ground state $\langle\mathbf{S}_\mu\rangle$ (more details in Appendix B), and iterate until the magnetization $\mathbf{m}_\mu$ at each site converges. It is equivalent to optimize the ground-state energy functional $E(\mathbf{m}_\mu) = \langle\Psi(\mathbf{m}_\mu)|\mathcal{H}_{\rm MF}|\Psi(\mathbf{m}_\mu)\rangle/\langle\Psi(\mathbf{m}_\mu)|\Psi(\mathbf{m}_\mu)\rangle$ variationally.

We would like to discuss one special case: the ground state supporting "collinear" magnetization orders. Namely, the magnetization vectors on the three sublattices are "parallel" or "antiparallel" to each other. It can be checked by investigating the angle $\theta_{<\mathbf{m}_\mu,\mathbf{m}_\nu>}$ between the two vectors $\mathbf{m}_\mu$ and $\mathbf{m}_\nu$ in (N^2-1)-dimensional spin space: $\theta_{<\mathbf{m}_\mu,\mathbf{m}_\nu>} = \arccos\frac{\mathbf{m}_\mu\cdot\mathbf{m}_\nu}{|\mathbf{m}_\mu||\mathbf{m}_\nu|}$, where the inner product and the norm are defined in (N^2-1)-dimensional generalized Euclidean space: $\mathbf{m}_\mu\cdot\mathbf{m}_\nu = \sum_{a=1}^{N^2-1} m_\mu^a m_\nu^a$, and $|\mathbf{m}_\mu| = \sqrt{\mathbf{m}_\mu\cdot\mathbf{m}_\mu}$. If $\cos\theta_{<\mathbf{m}_\mu,\mathbf{m}_\nu>} = \pm 1$, it implies that the two vectors $\mathbf{m}_\mu$ and $\mathbf{m}_\nu$ are collinear.

The reason why we discuss the special case of collinear magnetic orders is that, in such a case we can perform a *global* SU(N) unitary transformation to Eq. (6) to make some simplifications,

$$\mathbf{U}\mathbf{m}_\mu\cdot\boldsymbol{\tau}\mathbf{U}^\dagger = \sum_{a=1}^{N-1} m'^a\mathbf{H}^a, \tag{9}$$

in which $\mathbf{H}^a$ is the diagonal and commuting generator in SU(N) algebra and all the $\mathbf{H}^a$ constitute the Cartan subalgebra of SU(N) Lie algebra [40]: $\{\mathbf{H}^a, a = 1,2,\cdots,N-1\}$. Note that the Cartan subalgebra for SU(2) algebra is $\{\mathbf{H}^1 = T^3\}$, and for SU(3) algebra is $\{\mathbf{H}^1 = T^3, \mathbf{H}^2 = T^8\}$. Equation (9) can be understood in this way: the N dimensional Hermitian matrix $\mathbf{m}_\mu\cdot\boldsymbol{\tau}$ can be diagonalized by an SU(N) transformation $\mathbf{U}$; as $\mathbf{m}_\mu\cdot\boldsymbol{\tau}$ is traceless and this property is not changed by unitary transformations, the diagonalized matrix is also traceless; therefore, there are only $N-1$ degrees of freedom in the diagonalized matrix and it can be expanded by $N-1$ elements in Cartan subalgebra.

This important observation can not only significantly reduce the computational time, but also imply that there should be N degenerate equivalent mean-field ground states if the ground state supports collinear magnetic orders. These N equivalent mean-field states are determined by the N common eigenstates of the $N-1$ commuting generators in the Cartan subalgebra. As these

equivalent mean-field states are related to each other through SU(N) rotations, they are equivalent candidates for the spontaneous SU(N) symmetry breaking states. One could arbitrarily choose one of these N states to study the magnetic properties. These equivalent state can be understood with the aid of weights diagram in $\{\mathbf{H}^a, a = 1, 2, \cdots, N-1\}$ plane (see detailed discussions in Sec. VI). Take our familiar SU(2) models as an example: with SU(2) symmetry spontaneous breaking, the two equivalent ground states are the two eigenstates of σ_z, and it is the sign of self-consistent field that labels the ground state broken to spin-up polarized state or spin-down polarized state. In the conventional SU(2) case with collinear magnetic orders, one usually do analysis through considering only the z component of magnetic order parameter, where the x and y components are zero. It is easy to see that Eq. (9) is a generalization of this SU(2) wisdom to the more general SU(N) case. One need note that for a system with non-collinear (chiral or spiral) magnetization orders, we could not do this simplification because one can not find a *global* transformation that satisfies Eq. (9).

V. MEAN-FIELD CALCULATION FOR SU(2) HUBBARD MODEL

It is straightforward to perform the mean-field calculation for SU(2) Hubbard model, based on the general formulae derived for SU(N) Hubbard model. We take $N = 2$ and $\boldsymbol{\tau} = \boldsymbol{\sigma}$ into Eq. (8) and perform self-consistent iterations as specified in the previous section.

To verify how well the mean-filed calculation works, we first investigate the magnetization orders $\mathbf{m}_\mu$ at half-filling (filling fraction $\nu = 1$, which is defined as $\nu = N_e/N_s$, where N_e is the number of electrons and N_s is the number of sites). We find that the ground state has a collinear magnetic order at half filling for any value of U/t: $\mathbf{m}_\mathrm{B}$ is always parallel with $\mathbf{m}_\mathrm{C}$, and antiparallel with $\mathbf{m}_\mathrm{A}$ to minimize the ground-state energy. Namely, we do not find chiral or spiral magnetic order at half filing. And $\mathbf{m}_\mathrm{B} = \mathbf{m}_\mathrm{C}$ holds for any value of U/t, implying the C_4 symmetry is preserved. Since the magnetic order is collinear, we can perform a global SU(2) transformation, such that only m^z component is nonzero in the new axes in spin space. Therefore, we plot m^z_A, $m^z_\mathrm{B(C)}$ and total magnetization in one unit cell m^z_tot with increasing U/t in Fig. 2(a), where $m^{x,y}_\mu = 0$ after a global SU(2) rotation. The total magnetization in one unit cell is defined as $\mathbf{m}_\mathrm{tot} = \sum_{\mu=\mathrm{A,B,C}} \mathbf{m}_\mu$.

From Fig. 2(a), we find m^z_tot in one unit cell is 1/2 for any U/t, therefore the total magnetization on whole lattice is $\mathcal{N}/2$, where $\mathcal{N}$ is the number of unit cells. It implies that the SU(2) symmetry spontaneously breaks in the ground state, resulting in a ferromagnetic state. Recalling Lieb's theorem [7] that proves the weak interacting limit is adiabatically connected to the strong interacting limit, and the total spin is $\mathcal{N}/2$, which is independent of U/t, our mean-field calculation is consistent with Lieb's rigorous results. Another degenerate ground state with magnetization $-1/2$ per unit cell is found as expected, which is physically equivalent to the one with positive magnetization shown in Fig. 2(a). Therefore, it suffices to focus on the one with positive magnetization in the following discussion.

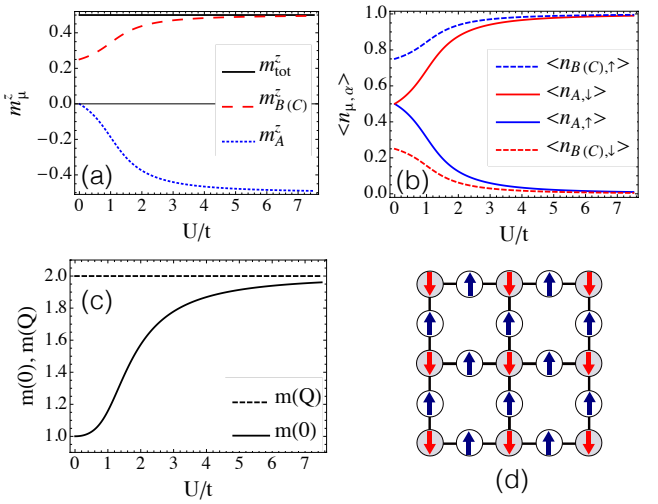

FIG. 2. (a) The magnetization orders on each site m^z_μ and total magnetization in one unit cell m^z_tot as functions of U/t, where μ = A,B,C. The result of $m^{x,y}_\mu$ is not shown due to $m^{x,y}_\mu = 0$. (b) The particle number of each spin component on each site $\langle n_{\mu,\alpha}\rangle$ as a function of U/t, where $\alpha = \uparrow, \downarrow$. (c) The correlation functions $m(0)$ and $m(Q)$. (d) A schematic figure showing the staggered ferromagnetic long-range order on the Lieb lattice for SU(2) Hubbard model at large U limit with half filling.

To see the contribution to magnetization comes from which sublattice, we plot the number of spin-up particles and spin-down particles at each site $\langle n_{\mu,\alpha}\rangle$, as a function of U/t in Fig. 2(b). We find the contribution from each sublattice depends on U/t. At weak interacting limit, the contribution to magnetization mainly comes from the particles on sublattices B and C. This behavior is close to the non-interacting case in which particles residing on sublattices B and C fill the flat band and contribute to magnetization. This is because in the non-interacting case, the wave function of zero energy state is $\psi(\boldsymbol{k}) \propto (0, -\cos(k_x), \cos(k_y))^T$, which implies the localized state residing on sublattices B and C. At large U limit, we find $m^z_\mathrm{A} = -1/2$, $m^z_\mathrm{B} = m^z_\mathrm{C} = 1/2$, and $\langle n_{\mathrm{A},\downarrow}\rangle = \langle n_{\mathrm{B},\uparrow}\rangle = \langle n_{\mathrm{C},\uparrow}\rangle = 1$. Namely, site A is occupied by one spin-down particle, while sites B and C are occupied by one spin-up particle, respectively. It reflects staggered ferromagnetic ordering and the Mott insulating picture, which is shown in Fig. 2(d) schematically.

Moreover, the ferromagnetic ground state can be identified from spin-density mean fields, i.e., the number of particles with spin α in one unit cell, defined as $\langle n_\alpha\rangle = \sum_{\mu=\mathrm{A,B,C}} \langle n_{\mu,\alpha}\rangle$. Although $\langle n_{\mu,\alpha}\rangle$ varies with

U/t in Fig. 2(b), the total number of particles of each spin in one unit cell $\langle n_\alpha \rangle$ is independent of U/t. Furthermore, we find $\langle n_\uparrow \rangle = 2\langle n_\downarrow \rangle$ for any $U > t$. Namely, the number of spin-up particles is twice the number of spin-down particles in every unit cell. This is another implication of ferromagnetic state.

We further analyze the correlation functions defined as

$$m(0) = \frac{1}{\mathcal{N}} \langle (\sum_i S_i^+)(\sum_j S_j^-) \rangle,$$
$$m(Q) = \frac{1}{\mathcal{N}} \langle (\sum_i \epsilon(i) S_i^+)(\sum_j \epsilon(j) S_j^-) \rangle, \qquad (10)$$

where the spin raising and lowering operators are defined as $S_i^+ = c_{i,\uparrow}^\dagger c_{i,\downarrow}$ and $S_i^- = c_{i,\downarrow}^\dagger c_{i,\uparrow}$, respectively, $\epsilon(i) = 1$ when site i belongs to sublattice A, and $\epsilon(i) = -1$ when site i belongs to sublattices B and C. Results of $m(0)$ and $m(Q)$ in the mean-field ground state as functions of U/t are shown in Fig. 2(c), showing respectively the existence of ferromagnetic long-range order and the staggered features therein. Notice that the relation $m(Q) \geq m(0)$ holds in our mean field calculation, which is consistent with the rigorous theorem [41].

In time-of-flight experiment, by tuning the laser power, the optical lattice potential can be dynamically controlled and adiabatically removed. During this adiabatic process, each Bloch wave is mapped to a free-particle momentum state [42]. Such band mapping technique can be used to probe particle's quasi-momentum distribution [42–44]. To compare with the particle absorbing image in time-of-flight experiment, we plot the band structure and show the particle filling of the lowest three bands, at zero temperature with different interactions, as shown in Fig 3: (a) $U/t = 0.1$, (b) $U/t = 0.5$, (c) $U/t = 1.5$ and (d) $U/t = 5.0$. We find at half filling, the first, the second and the third bands are occupied by spin-up, spin-down, and spin-up particles, respectively.

Since the Lieb's theorem [7] only works at half filling ($\nu = 1$), we want to go beyond this filling and observe the relation between magnetization and filling fraction ν, where $2/3 \leq \nu \leq 4/3$. In this range, the flat band is partially filled in non-interacting picture. Since in the non-interacting limit, the particles filling flat band contribute to magnetization, we expect this picture still holds in the weak-interacting limit. If this is true, the magnetization is expected to be proportional to the filling fraction when $2/3 \leq \nu \leq 4/3$ and $U/t \ll 1$. We find in this filling range, the magnetization indeed grows with increasing filling fraction as shown in Fig. 4, which means at such filling, once the flat band in corresponding non-interacting limit is filled by particles, the magnetization of the interacting model is nonzero. It seems to contradict with a previous study [45], that takes Tasaki lattice [5, 6] as an example, maps the flat band ferromagnetism to Pauli-correlated percolation problem and shows ferromagnetism appears above some critical filling to the flat band. The Tasaki lattice can be regarded as Lieb lattice with introduced nearest-neighbor hoppings among sublattice A, in which

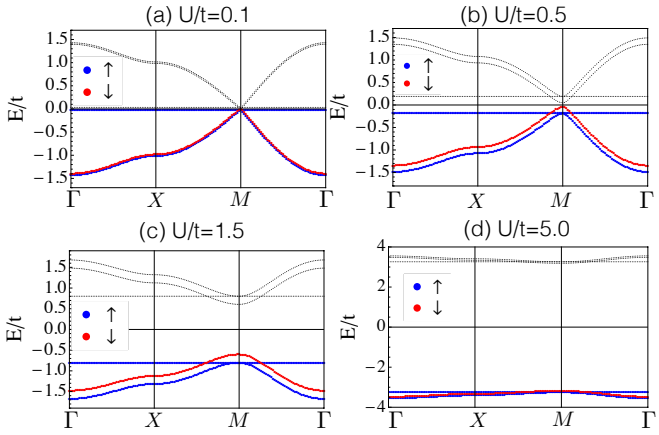

FIG. 3. The band structure at zero temperature with different interactions: (a) $U/t = 0.1$, (b) $U/t = 0.5$, (c) $U/t = 1.5$ and (d) $U/t = 5.0$. The band filled by spin-up (down) particles is labeled in blue (red).

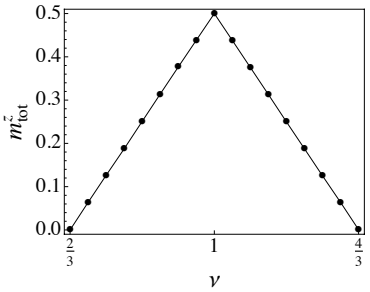

FIG. 4. The total magnetization in one unit cell $m_{\rm tot}^z$ as a function of filling fraction ν with $U/t = 0.505$. Similar to the half-filling case, the magnetization orders are collinear: $\mathbf{m}_{\rm B}$ is parallel with $\mathbf{m}_{\rm C}$ and antiparallel with $\mathbf{m}_{\rm A}$, where $\mathbf{m}_{\rm B} = \mathbf{m}_{\rm C}$. Therefore, we only plot total magnetization in one unit cell $m_{\rm tot}^z$ ($m_{\rm tot}^{x,y} = 0$ and is not shown).

case the bipartiteness breaks down. As a result, the lowest band is tuned to be flat. Thus, the method of mapping magnetization to Pauli-correlated percolation, which requires the number of particles per trapping cell is no more than one [45], does not apply to the Lieb lattice problem discussed here, since the number of particles per trapping cell is more than two when the flat band is partially filled.

Finally, we consider the residual symmetry of SU(2) Hubbard model in the ferromagnetic phase. When SU(2) symmetry breaks, resulting in a two-fold degenerate ferromagnetic ground state, the U(1) symmetry still remains, where the charge of each spin component is conserved. The symmetry breaking is thus SU(2) $\rightarrow$ U(1).

To conclude, we notice the mean-field calculation works well to capture the magnetic properties of the ground state for SU(2) Hubbard model. We find at half filling, the SU(2) symmetry is spontaneously broken into U(1) symmetry in the ground state, resulting in a ferromagnetic state, in which the magnetization in one unit

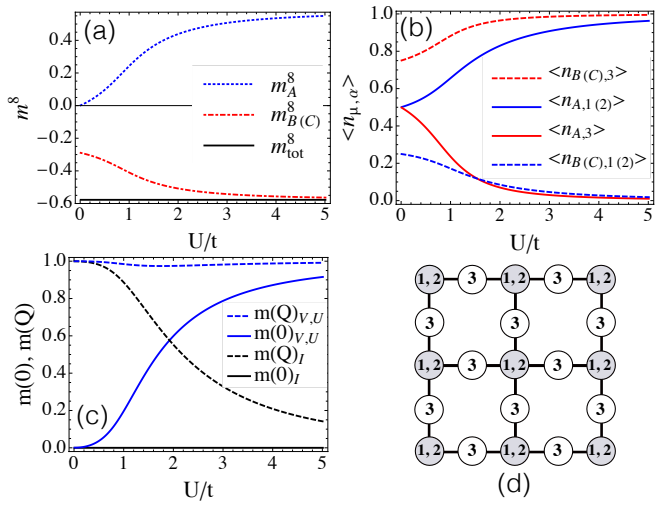

FIG. 5. (a) Results of $m^8_{\mathrm{A,B(C)}}$ and m^8_{tot} in one unit cell as functions of U/t. (b) The particle numbers on each site with different flavors $\langle n_{\mu,\alpha}\rangle$. (c) The correlation functions $m(0)_{I,V,U}$ and $m(Q)_{I,V,U}$ as functions of U/t. (d) A schematic figure showing the flavor-density distribution and the staggered ferromagnetic long-range order on the Lieb lattice for SU(3) Hubbard model at large U limit with 4/9 filling.

cell is 1/2. The total magnetization is found to be independent of interaction. Our mean field calculation is qualitatively consistent with the conclusions obtained by Lieb's theorem. Moreover, we find it supports the staggered ferromagnetic long-range order, which is consistent with Ref. 41. The picture that particles filling the flat band contribute to magnetization works well, at least in the weak interacting limit for SU(2) Hubbard model.

VI. FERROMAGNETIC GROUND STATE OF SU(3) HUBBARD MODEL

For the Hubbard model with SU(3) symmetry, there are three species of particles, hence we take $\alpha = 1, 2, 3$ to label the flavors or colors of the particles. As the ferromagnetic state may correspond to particles partially filling the flat band in the non-interacting case, here we consider a typical example of 4/9 or 5/9 filling (the filling fraction $\nu = 4/3$ or $5/3$). We then take $N = 3$, and $\boldsymbol{\tau} = \boldsymbol{\lambda}$ (λ^a is a Gell-Mann matrix in fundamental representation (see Appendix A), $a = 1, \cdots, 8$) into Eq. (8) and solve the problem self-consistently.

The magnetization order $\mathbf{m}_\mu$ now is an eight-dimensional vector in spin space, which transforms according to the adjoint represent of SU(3) Lie algebra. We find that at 4/9 filling the ground state supports a collinear magnetic order, because $\cos\theta_{<\mathbf{m}_{\mathrm{A}},\mathbf{m}_{\mathrm{B(C)}}>} = -1$ is found numerically. One way to investigate the collinear magnetization orders in eight-dimensional space is considering the norm of total magnetization in one unit cell $|\mathbf{m}_{\mathrm{tot}}|$. We find $|\mathbf{m}_{\mathrm{tot}}| = 1/\sqrt{3}$, which implies the ground state is ferromagnetic. Another more comprehensive way to analyze the collinear magnetization orders is performing a global SU(3) transformation to the mean-field Hamiltonian, so that the ferromagnetic ground states are denoted by $|m^3_{\mathrm{tot}}, m^8_{\mathrm{tot}}\rangle$ as explained at the end of Sec. IV, where the other six components of $\mathbf{m}_{\mathrm{tot}}$ are zeroes. We indeed find the ferromagnetic ground state has three-fold degeneracy as expected, which can be labeled by $|0, -1/\sqrt{3}\rangle$ and $|\pm 1/2, 1/2\sqrt{3}\rangle$. These three degenerate states are physically equivalent and can be transformed to each other by an SU(3) rotation as discussed before. Therefore, it suffices to focus on any one of them. Without loss of generality, we choose the one described by $|0, -1/\sqrt{3}\rangle$ in the following, whose magnetization in one unit cell is denoted by $(m^3 = 0, m^8 = -1/\sqrt{3})$.

To see how magnetization is affected by interaction and distributed on different sublattices, we plot $m^8_{\mathrm{A,B(C)}}$ and m^8_{tot} as functions of U/t in Fig. 5(a). The components associated with $m^3_{\mu=\mathrm{A,B,C}}$ are zero in the ground state hence are not shown. The C_4 symmetry is preserved for any finite U due to $m^8_{\mathrm{C}} = m^8_{\mathrm{B}}$. Similar to the SU(2) case, the ground state of SU(3) Hubbard model is ferromagnetic with collinear magnetic orders for any finite $U/t > 0$. And the values of magnetization m^3 and m^8 are independent of U/t. Namely, the ferromagnetic ground state at weak-interacting limit is adiabatically connected to the one at strong-interacting limit. The ferromagnetic state implies the spontaneous SU(3) symmetry breaking in the presence of finite U.

We plot the numbers of particles with different flavors at each site $\langle n_{\mu,\alpha}\rangle$ as functions of U/t in Fig. 5(b) to show the contribution to magnetization from different sublattices. We find the number of particles with flavor 1 is the same as that with flavor 2 on each sublattice, $\langle n_{\mu,1}\rangle = \langle n_{\mu,2}\rangle$. It is a consequence of residual symmetry created by SU(3) symmetry breaking and will be discussed later. Similar to the SU(2) systems, at the weak-interacting limit, the contribution to magnetization mainly comes from particles residing on sublattice B and C. But at large U limit, we find $m^8_{\mathrm{A}} = \sqrt{3}/3$, $m^8_{\mathrm{B(C)}} = -\sqrt{3}/3$ and $n_{\mathrm{A},1(2)} = 1$, $n_{\mathrm{B(C)},3} = 1$. Namely, site A is occupied by two particles with flavor-1 and flavor-2 , while sites B and C are occupied by one flavor-3 particle, respectively. A schematic figure to illustrate the flavor-density distribution pattern of SU(3) Hubbard model at 4/9 filling on the Lieb lattice is shown in Fig. 5(d). In the intermediate interaction range, the flavor-density pattern can be summarized as: particles with two flavors (flavor-1 and 2) prefer one sublattice (A) with equal density, while the particles with the third flavor (flavor-3) prefer the other sublattice (B and C actually belong to the same sublattice as C_4 symmetry is preserved here) with a larger density.

The property that the ground state is ferromagnetic can also be obtained by noticing the imbalanced number of particles with different flavors from the flavor-density mean fields $\langle n_\alpha\rangle$. We find that $\langle n_1\rangle = \langle n_2\rangle = 1$ and $\langle n_3\rangle = 2$ in one unit cell. And the expectation value of

particle number in each spin component in the ground state is independent of U/t. Such a fact implies a ferromagnetic state, which exists at any finite U.

We also investigate the long-range correlations in the ground state of the SU(3) Hamiltonian. Different from the SU(2) system, we need to define three pairs of "spin-raising" and "spin-lowering" operators [40]: $I^{\pm} \equiv T^1 \pm iT^2 = E_{\pm 1,0}$, $V^{\pm} \equiv T^4 \pm iT^5 = E_{\pm 1/2,\pm\sqrt{3}/2}$, $U^{\pm} \equiv T^6 \pm iT^7 = E_{\mp 1/2,\pm\sqrt{3}/2}$, where $T^{\alpha} = \lambda^{\alpha}/2$. Then we define three pairs of correlation functions as

$$m(0)_O = \frac{1}{\mathscr{N}}\langle (\sum_i O_i^+)(\sum_j O_j^-)\rangle,$$
$$m(Q)_O = \frac{1}{\mathscr{N}}\langle (\sum_i \epsilon(i) O_i^+)(\sum_j \epsilon(j) O_j^-)\rangle,$$

where $O = I, V, U$, $\epsilon(i) = 1$ when $i \in A$, and $\epsilon(i) = -1$ when $i \in B(C)$. The plots of $m(0)_O$ and $m(Q)_O$ in the mean-field ground state as functions of U/t are shown in Fig. 5 (c). We find in the ferromagnetic ground state denoted by $|0, -\frac{1}{\sqrt{3}}\rangle$, the correlation functions $m(0)_{V,U}$ and $m(Q)_{V,U}$ are nonzero, implying the ferromagnetic long-range order and staggered features therein as well. Besides, we find that the relation $m(Q)_O \geq m(0)_O$ still holds in our mean field calculation.

Now we discuss the residual symmetry in the ground state resulted by an SU(3) symmetry breaking. There are three equivalent ferromagnetic states in which the SU(3) symmetry could spontaneously break. For each of these three ground states, there still exists a residual SU(2)×U(1) symmetry. One could understand this with the help of weights diagram of SU(3)(see Fig. 6(b)). For example, if $|0, -1/\sqrt{3}\rangle$ is chosen as the mean-field ferromagnetic ground state, one could see that [40]

$$I^+|0, -\frac{1}{\sqrt{3}}\rangle = 0,$$
$$I^-|0, -\frac{1}{\sqrt{3}}\rangle = 0.$$

That is to say, there is an SU(2) symmetry with generators $\{T^1, T^2, T^3\}$ which leaves the mean-field ground state invariant. The extra U(1) symmetry is the usual charge conservation symmetry. In the general SU(N) case, there would be N equivalent ferromagnetic states in which the SU(N) symmetry could spontaneously break and the symmetry breaking pattern would be SU(N) → SU($N-1$)×U(1).

Furthermore, to compare with the absorbing image in time-of-flight experiment, we plot the band structure and label the lowest four bands with the flavors of particles filling the bands with different interactions as shown in Fig 7: (a) $U/t = 0.1$, (b) $U/t = 0.5$, (c) $U/t = 1.5$, and $U/t = 5.0$. We find there are three double-degenerate bands, which degenerate in flavor-1 and flavor-2. With weak interaction as shown in Figs. 7(a) and 7(b), the first and the forth bands are occupied by flavor-3 particles; the second and third bands (degenerate) are occupied

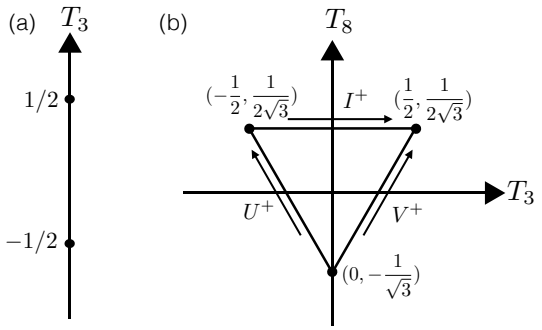

FIG. 6. The equivalent ferromagnetic ground state can be shown with the aid of weights diagram of (a) SU(2) Lie algebra and (b) SU(3) Lie algebra. The coordinates of the weights are labeled in each diagram.

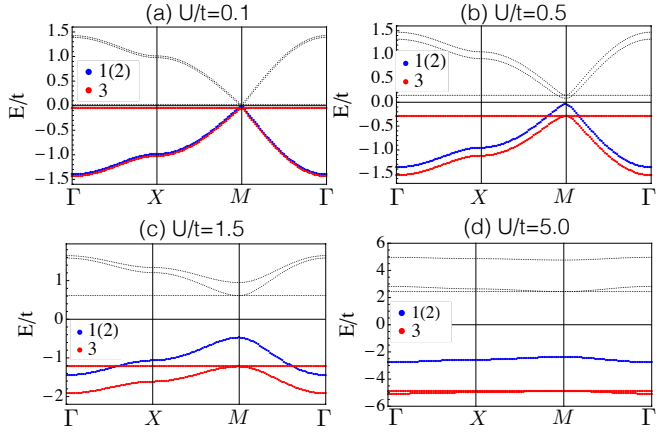

FIG. 7. The band structure at zero temperature with different interactions (a) $U/t = 0.1$, (b) $U/t = 0.5$, (c) $U/t = 1.5$ and (d) $U/t = 5.0$. The band filled by flavor-1 or flavor-2 particles is labeled in blue, while the band filled by flavor-3 particles is labeled in red.

by flavor-1 and flavor-2 particles, respectively. This observation indicates that in this weakly interacting case, one can still rely on the particle-filling picture in which the particles residing on the flat band contribute to the magnetization.

However, at large U limit as shown in Fig. 7(d), we find the lowest two bands are occupied by flavor-3 particles, and the particles with flavor-1 and flavor-2 occupy two higher bands. This is because at large U limit, particles with flavor-1 and flavor-2 residing on the same sublattice A as shown in Fig. 5(d) obtain a much larger interaction energy comparing with kinetic energy. Therefore, the particles with flavor-1 and flavor-2 can populate into higher bands, due to the higher energy gained by the interaction. We find the flavor distribution in quasi-momentum space is sensitive to interactions. This observation could by observed in time-of-flight expansion by adiabatic removal of trapping potential [44].

In addition, we find that the system is an insulator

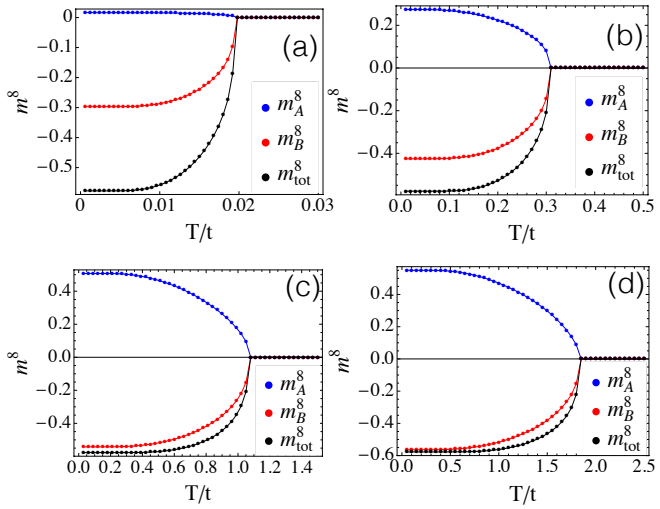

FIG. 8. The magnetization at finite temperature with different interactions: (a) $U/t = 0.11$, $T_c/t = 0.0198$; (b) $U/t = 1.11$, $T_c/t = 0.32$; (c) $U/t = 3.01$, $T_c/t = 1.11$ and (d) $U/t = 5.01$, $T_c/t = 1.9$.

with a finite gap in the ground state. The presence of such a gap is allowed by generalized Lieb-Schultz-Mattis (LSM) theorem [46]. The original LSM theorem proves the excitation gap in antiferromagnetic spin chain [47]. It is later extended in a quantum many-particle system (bosons or fermions) with translational symmetry preserved and with conserved particle number, where a finite excitation gap is proved to be possible only if the number of particles per unit cell is an integer in the ground state [46]. In our settings, the particle number per unit cell is an integer, and we find the particle number of each flavor component in the ground state $\langle n_\alpha \rangle$ is an integer as well. Therefore, the gap found in our SU(3) system is consistent with the generalized LSM theorem [46].

Finally, we plot the magnetization as a function of temperature with different values of interaction in Fig. 8. Although Mermin-Wagner theorem forbids the existence of any long-range order with short-range interaction in two-dimensional system at finite temperatures [48, 49], there may be some quasi long-range order. Our mean-field calculation estimate the ferromagnetic ordering is destroyed by thermal fluctuation, but the remaining quasi long-range order can persist to a finite temperature. The critical temperature T_c increases with increasing $U/$t. Therefore, in experiment the ferromagnetic ground state could be observed in cold atomic systems loaded into an optical lattice with increasing density-density on-site interaction.

In summary, we extend the mean-field calculation for the SU(3) Hubbard model on the Lieb lattice. We find that at 4/9 filling, which corresponds to that the flat band is 1/3 filled in the non-interacting case, the ground state is ferromagnetic and supports a collinear magnetic order. We find the SU(3) symmetry breaks into SU(2)×U(1) symmetry, supporting a staggered ferromagnetic long-range order. The staggered ferromagnetic quasi long-range order can persist at finite temperature and may be observed as magnetic domains in absorbing images, with increasing interaction.

VII. CONCLUSIONS AND DISCUSSIONS

In conclusion, we have studied the magnetic properties of SU(2) and SU(3) Hubbard models at the mean field level, by solving the mean-field self-consistent equations. We find the mean-field calculation works well to capture the magnetic properties of the ground state of SU(2) Hubbard model. At half filling, the ground state of SU(2) Hubbard model is ferromagnetic for any interaction $U > 0$, which is consistent with known rigorous results. In the ferromagnetic ground state, the SU(2) symmetry breaks into U(1) symmetry. We then extend the mean-field calculation for SU(3) Hubbard model on the Lieb lattice. We find at 4/9 filling, SU(3) symmetry spontaneously breaks into SU(2)× U(1) symmetry. The ground state is ferromagnetic for any finite $U > 0$ with magnetization orders labeled by $m_0(0, -1)$ and $m_0(\pm\sqrt{3}/2, 1/2)$, where m_0 is found to be $\sqrt{3}/3$. The band structure with flavored particles filling suggests the magnetic domains and flavor distribution in quasi momentum space could be observed in time-of-flight experiment by band mapping technique. The staggered ferromagnetic quasi long-rang order is destroyed by thermal fluctuation, and the quasi long-range order can persist to a finite temperature. Since the critical temperature increases with interactions, the magnetic domains in absorbing image could be observed at an experimentally achievable temperature by increasing the density-density interaction.

VIII. ACKNOWLEDGEMENT

We thank H. Zhai suggesting this interesting and important problem to us and appreciate the insightful discussion and early collaboration with him. We thank helpful discussion with M. Oshikawa, Z.-X. Liu, W. Chen, W. Zheng, L.-Y. Wang, R.-Q. He and Z.-X. Li. W.-X. Nie acknowledges the support of International Postdoc Exchange Program from China. W. Z. is supported by NSFC (11274009, 11434011, 11522436), NKBRP (2013CB922000) and the Research Funds of Renmin University of China (10XNL016, 16XNLQ03).

Appendix A: Gell-Mann matrices

The Gell-Mann matrices we used in three-dimensional fundamental representation are:

$$\lambda^1=\begin{pmatrix}0&1&0\\1&0&0\\0&0&0\end{pmatrix},\lambda^2=\begin{pmatrix}0&-i&0\\i&0&0\\0&0&0\end{pmatrix},\lambda^3=\begin{pmatrix}1&0&0\\0&-1&0\\0&0&0\end{pmatrix},$$

$$\lambda^4=\begin{pmatrix}0&0&1\\0&0&0\\1&0&0\end{pmatrix},\lambda^5=\begin{pmatrix}0&0&-i\\0&0&0\\i&0&0\end{pmatrix},\lambda^6=\begin{pmatrix}0&0&0\\0&0&1\\0&1&0\end{pmatrix},$$

$$\lambda^7=\begin{pmatrix}0&0&0\\0&0&-i\\0&i&0\end{pmatrix},\lambda^8=\frac{1}{\sqrt{3}}\begin{pmatrix}1&0&0\\0&1&0\\0&0&-2\end{pmatrix}.$$

Appendix B: Technical part of general mean-field approach for SU(N) Hubbard model

In the presence of repulsive interaction, the model on the two-dimensional Lieb lattice can not be exactly solved. And we resort to mean-field approximation. For the magnetic properties of the ground state, we rewrite the density-density interaction in spin channel first. Considering the traceless property of the SU(N) generators $\mathrm{Tr}\ T^a=0$ and $\mathrm{Tr}(T^aT^b)=\delta_{ab}/2$, the completeness relation of the generators is obtained:

$$\sum_{a=1}^{N^2-1}T^a_{\alpha\beta}T^a_{\mu\nu}=\frac{1}{2}\delta_{\alpha\nu}\delta_{\beta\mu}-\frac{1}{2N}\delta_{\alpha\beta}\delta_{\mu\nu}. \tag{B1}$$

Applying the completeness relation, we obtain following identity

$$\mathbf{S}_i^2=(N+1)n_i/2-(N+1)n_i^2/(2N). \tag{B2}$$

Therefore, the density-density interaction is rewritten as Eq. (5).

The matrix $H^{\mathrm{MF}}_{\mathbf{k}}$ in Eq. (8) can be diagonalized by a unitary transformation $U(\mathbf{k})H^{\mathrm{MF}}_{\mathbf{k}}U^\dagger(\mathbf{k})=\Lambda_{\mathbf{k}}$, where $\Lambda_{\mathbf{k}}$ is a diagonal matrix, $\Phi_{\mathbf{k}}=U(\mathbf{k})\Gamma_{\mathbf{k}}$, and $\Gamma_{\mathbf{k}}=(\gamma_1(\mathbf{k}),\cdots,\gamma_{3N}(\mathbf{k}))^T$. We then obtain $3N$ energy bands with eigenvalues $E_m(\mathbf{k})$ ($m=1,\cdots,3N$), and corresponding eigenfunctions. For a fixed filling fraction, the wavefunction at zero temperature is defined as

$$|\mathrm{GS}\rangle=\prod_{\mathbf{k}\in\mathrm{BZ}}\prod_{m|E_m(\mathbf{k})\le E_F}\gamma^\dagger_m(\mathbf{k})|0\rangle. \tag{B3}$$

In the self-consistent mean-field calculation, we need to calculate the magnetization at each iteration step, which is defined as the expectation value of spin operator in the ground state:

$$\begin{aligned}m^a_\mu&=\langle S^a_\mu(\mathbf{R})\rangle=\sum_{\alpha\beta}\langle c^\dagger_{\mu,\alpha}(\mathbf{R})\frac{\tau^a_{\alpha\beta}}{2}c_{\mu,\beta}(\mathbf{R})\rangle\\&=\frac{1}{2\mathscr{N}}\sum_{\mathbf{k}\in\mathrm{BZ}}\sum_{\alpha\beta}\langle c^\dagger_{\mu,\alpha}(\mathbf{k})\tau^a_{\alpha\beta}c_{\mu,\beta}(\mathbf{k})\rangle,\end{aligned} \tag{B4}$$

where the translation symmetry is assumed. Equation (B4) is the self-consistent equation for the mean-field calculation. We can write the matrix form of the unitary transformation of $U(\mathbf{k})$, $c_{\mu,\alpha}(\mathbf{k})=\sum_m U_{\mu,\alpha,m}(\mathbf{k})\gamma_m(\mathbf{k})$. With the definition of the ground state in Eq. (B3), we find that

$$\begin{aligned}&\langle c^\dagger_{\mu,\alpha}(\mathbf{k})c_{\mu,\beta}(\mathbf{k})\rangle_{\mathrm{GS}}\\&=\sum_{mn}U^*_{\mu,\alpha,m}(\mathbf{k})U_{\mu,\beta,n}(\mathbf{k})\langle\mathrm{GS}|\gamma^\dagger_m(\mathbf{k})\gamma_n(\mathbf{k})|\mathrm{GS}\rangle\\&=\sum_{m|E_m(\mathbf{k})\le E_F}U^*_{\mu,\alpha,m}(\mathbf{k})U_{\mu,\beta,m}(\mathbf{k}).\end{aligned} \tag{B5}$$

[1] E. Lieb and D. Mattis, Phys. Rev. **125**, 164 (1962).
[2] Y. Nagaoka, Phys. Rev. **147**, 392 (1966).
[3] A. Mielke, J. Phys. A: Math. Gen. **24**, L73 (1991).
[4] A. Mielke, J. Phys. A: Math. Gen. **24**, 3311 (1991).
[5] H. Tasaki, Phys. Rev. Lett. **69**, 1608 (1992).
[6] A. Mielke and H. Tasaki, Commun. Math. Phys. **158**, 341 (1993).
[7] E. H. Lieb, Phys. Rev. Lett. **62**, 1201 (1989).
[8] Y. Li, E. H. Lieb, and C. Wu, Phys. Rev. Lett. **112**, 217201 (2014).
[9] D. J. Thouless, Proc. Phys. Soc. **86**, 893 (1965).
[10] I. Affleck and J. B. Marston, Phys. Rev. B **37**, 3774 (1988).
[11] J. B. Marston and I. Affleck, Phys. Rev. B **39**, 11538 (1989).
[12] N. Read and S. Sachdev, Phys. Rev. B **42**, 4568 (1990).
[13] N. Read and S. Sachdev, Phys. Rev. Lett. **62**, 1694 (1989).
[14] C. Honerkamp and W. Hofstetter, Phys. Rev. Lett. **92**, 170403 (2004).
[15] A. Rapp, G. Zaránd, C. Honerkamp, and W. Hofstetter, Phys. Rev. Lett. **98**, 160405 (2007).
[16] A. V. Gorshkov, M. Hermele, V. Gurarie, C. Xu, P. S. Julienne, J. Ye, P. Zoller, E. Demler, M. D. Lukin, and A. M. Rey, Nat. Phys. **6**, 289 (2010).
[17] B. J. DeSalvo, M. Yan, P. G. Mickelson, Y. N. Martinez de Escobar, and T. C. Killian, Phys. Rev. Lett. **105**, 030402 (2010).
[18] F. Scazza, C. Hofrichter, M. Hofer, P. C. De Groot, I. Bloch, and S. Folling, Nat. Phys. **10**, 779 (2014).
[19] G. Pagano, M. Mancini, G. Cappellini, P. Lombardi, F. Schafer, H. Hu, X.-J. Liu, J. Catani, C. Sias, M. Inguscio, and L. Fallani, Nat. Phys. **10**, 198 (2014).
[20] T. Fukuhara, Y. Takasu, M. Kumakura, and Y. Taka-

hashi, Phys. Rev. Lett. **98**, 030401 (2007).
[21] S. Taie, R. Yamazaki, S. Sugawa, and Y. Takahashi, Nat. Phys. **8**, 825 (2012).
[22] R. Zhang, Y. Cheng, H. Zhai, and P. Zhang, Phys. Rev. Lett. **115**, 135301 (2015).
[23] G. Pagano, M. Mancini, G. Cappellini, L. Livi, C. Sias, J. Catani, M. Inguscio, and L. Fallani, Phys. Rev. Lett. **115**, 265301 (2015).
[24] M. Höfer, L. Riegger, F. Scazza, C. Hofrichter, D. R. Fernandes, M. M. Parish, J. Levinsen, I. Bloch, and S. Fölling, Phys. Rev. Lett. **115**, 265302 (2015).
[25] H. Katsura and A. Tanaka, Phys. Rev. A **87**, 013617 (2013).
[26] M. A. Cazalilla, A. F. Ho, and M. Ueda, New J. Phys. **11**, 103033 (2009).
[27] S. Taie, H. Ozawa, T. Ichinose, T. Nishio, S. Nakajima, and Y. Takahashi, Science Advances **1** (2015), 10.1126/sciadv.1500854.
[28] K.-J. Chen and W. Zhang, Chin. Phys. Lett. **31**, 110303 (2014).
[29] W.-F. Tsai, C. Fang, H. Yao, and J. Hu, New J. of Phys. **17**, 055016 (2015).
[30] N. Goldman, D. F. Urban, and D. Bercioux, Phys. Rev. A **83**, 063601 (2011).
[31] H. Wang, S.-L. Yu, and J.-X. Li, Phys. Lett. A **378**, 3360 (2014).
[32] K. Noda, A. Koga, N. Kawakami, and T. Pruschke, Phys. Rev. A **80**, 063622 (2009).
[33] K. Noda, K. Inaba, and M. Yamashita, Phys. Rev. A **90**, 043624 (2014).
[34] K. Noda, K. Inaba, and M. Yamashita, Phys. Rev. A **91**, 063610 (2015).
[35] A. Dauphin, M. Müller, and M. A. Martin-Delgado, Phys. Rev. A **93**, 043611 (2016).
[36] R. Shen, L. B. Shao, B. Wang, and D. Y. Xing, Phys. Rev. B **81**, 041410 (2010).
[37] V. Apaja, M. Hyrkäs, and M. Manninen, Phys. Rev. A **82**, 041402 (2010).
[38] A. Jaffe and F. Pedrocchi, Ann. Henri Poincar **16**, 189 (2015).
[39] Z. Li and H. Yao, (2015), private communications.
[40] G. Howard, *Lie Algebras In Particle Physics,From Isospin to Unified Theories*, 2nd ed. (Westview Press, 1999).
[41] S.-Q. Shen, Z.-M. Qiu, and G.-S. Tian, Phys. Rev. Lett. **72**, 1280 (1994).
[42] I. Bloch, J. Dalibard, and W. Zwerger, Rev. Mod. Phys. **80**, 885 (2008).
[43] M. Greiner, I. Bloch, O. Mandel, T. W. Hänsch, and T. Esslinger, Phys. Rev. Lett. **87**, 160405 (2001).
[44] M. Köhl, H. Moritz, T. Stöferle, K. Günter, and T. Esslinger, Phys. Rev. Lett. **94**, 080403 (2005).
[45] M. Maksymenko, A. Honecker, R. Moessner, J. Richter, and O. Derzhko, Phys. Rev. Lett. **109**, 096404 (2012).
[46] M. Oshikawa, Phys. Rev. Lett. **84**, 1535 (2000).
[47] E. H. Lieb, T. Schultz, and D. J. Mattis, Ann. Phys. (N. Y.) **16**, 407 (1961).
[48] N. D. Mermin and H. Wagner, Phys. Rev. Lett. **17**, 1133 (1966).
[49] N. D. Mermin, Phys. Rev. **176**, 250 (1968).